

Received:
09 January 2023

Revised:
21 March 2023

Accepted:
14 April 2023

© 2023 The Authors. Published by the British Institute of Radiology under the terms of the Creative Commons Attribution-NonCommercial 4.0 Unported License <http://creativecommons.org/licenses/by-nc/4.0/>, which permits unrestricted non-commercial reuse, provided the original author and source are credited.

Cite this article as:
Cundari G, Alkadhi H, Eberhard M. The role of CT in arrhythmia management—treatment planning and post-procedural imaging surveillance. *Br J Radiol* (2023) 10.1259/bjr.20230028.

REVIEW ARTICLE

The role of CT in arrhythmia management—treatment planning and post-procedural imaging surveillance

^{1,2}GIULIA CUNDARI, MD, ¹HATEM ALKADHI, MD, MPH, EBCR, FESER and ^{1,3}MATTHIAS EBERHARD, MD, EBCR

¹Diagnostic and Interventional Radiology, University Hospital Zurich, University of Zurich, Zurich, Switzerland

²Department of Radiological, Oncological and Anatomopathological Sciences, Sapienza University of Rome, Rome, Italy

³Department of Radiology, Spital Interlaken, Spitälerfmi AG, Unterseen, Switzerland

Address correspondence to: Dr Hatem Alkadhi
E-mail: hatem.alkadhi@usz.ch

ABSTRACT

Several interventional treatment options exist in patients with atrial and ventricular arrhythmia. Cardiac CT is routinely performed prior to occlusion of the left atrial appendage, pulmonary vein isolation, and cardiac device implantation. Besides the evaluation of coronary artery disease, cardiac CT provides isotropic, high-resolution CT images of the cardiac anatomy with the possibility of multiplanar reformations and three-dimensional reconstructions which are helpful to guide interventional treatment. In addition, cardiac CT is increasingly used to rapidly evaluate periprocedural complications and for the routine post-procedural imaging surveillance in patients after interventions. This review article will discuss current applications of pre- and post-interventional CT imaging in patients with arrhythmia.

INTRODUCTION

Interventional cardiac procedures play an important role in the treatment of patients with arrhythmia and in the prevention of complications from arrhythmia. Interventional occlusion of the left atrial appendage (LAA) is an alternative treatment approach in patients with atrial fibrillation (AF) in whom anticoagulation is contraindicated or ineffective.¹ Radiofrequency catheter ablation is an established treatment option in patients with AF as well as ventricular arrhythmia.² Cardiac resynchronization therapy (CRT) and implantable cardioverter defibrillator (ICD) implantation may reduce mortality in patients with sustained cardiac arrest or heart failure and mechanical dyssynchrony of the left and right ventricle.

Cross-sectional imaging is increasingly requested before these interventions.³ Cardiac CT has the advantage to provide non-invasive, isotropic, high-resolution images of the cardiac anatomy with the possibility of multiplanar reformations and three-dimensional (3D) reconstructions, facilitating treatment planning. CT is also the primary modality for the rapid evaluation of suspected procedure-related complications and increasingly used for post-procedural surveillance after cardiac interventions.

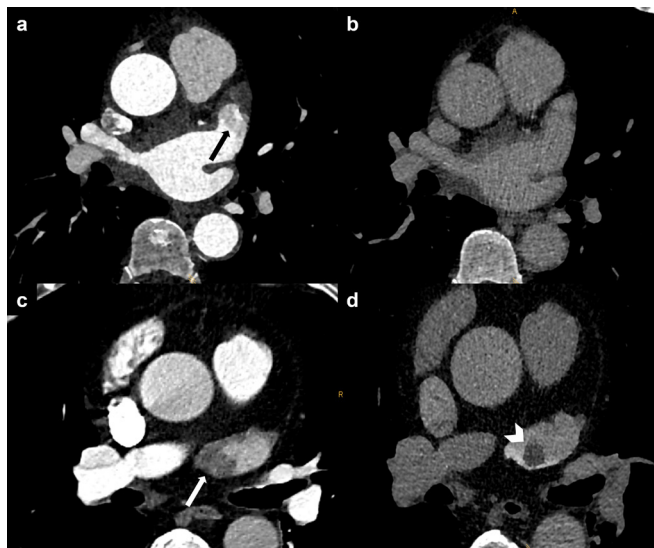
This article will review current applications of pre- and post-interventional CT imaging in LAA occlusion, pulmonary vein isolation and cardiac device implantation.

Cardiac CT imaging technique

Cardiac CT requires advanced CT scanner technology enabling high spatial and temporal resolution. A high temporal resolution enables cardiac CT imaging with less motion artifacts, particularly important when imaging patients with arrhythmia.⁴ Cardiac reconstruction algorithms typically utilize 180° of projection data, resembling a half gantry rotation for image reconstruction. In dual-source CT scanners with two X-ray sources positioned at approximately 90° to each other, sufficient data for image reconstruction can be acquired at one-fourth of a complete gantry rotation. This results in an intrinsic temporal resolution of around 115–135 ms for top-end single-source CT scanners and of around 65–75 ms for dual-source CT scanners.

The acquisition protocol for cardiac CT mainly depends on the available scanner. Prospective ECG-gating is often preferred in newer scanners to keep radiation dose levels low. For pre-procedural cardiac CT before pulmonary vein isolation or LAA occlusion, the acquisition window can be limited to end-systole, obtaining images at around 30–60% of the RR-interval.^{5,6} With older scanners or patients with

Figure 1. Ruling out LAA thrombus. (a) Filling defect of the LAA in the arterial phase being suspicious of thrombus (black arrow), (b) delayed phase after 60s showing normal opacification of the LAA. (c) Filling defect of the LAA in the arterial phase (white arrow). (d) Delayed phase after 60s showing a 1cm thrombus in the LAA (white arrowhead). LAA, left atrial appendage



variable and high heart rates, a retrospective spiral acquisition should be considered. ECG-based dose modulation (also called ECG pulsing) enables to limit the full tube current application to the end-systole which goes along with considerable reduction of the radiation dose also in this mode.⁷

Depending on the body habitus of the patient, the tube voltage can be reduced down to 70 kV or 80 kV to reduce radiation dose as well as to increase the attenuation of the cardiac chambers when scanning with a tube voltage closer to the k-edge of iodine. Recent technical development of dual-layer spectral detector CT and photon-counting CT further facilitate high contrast to noise ratios due to the possibility of monoenergetic image reconstruction of spectral CT data, yielding the potential for contrast media reduction.⁸

Misregistration between successively acquired CT slabs due to motion artifacts is an important issue in patients with arrhythmia. Acquiring the CT scan in one heartbeat reduces the likelihood of misregistration. Two possibilities are available: (i) scanning with a single-source detector with a detector array of ≥ 160 mm in the longitudinal z-axis covering the whole heart in one acquisition without the need for table movement and (ii) scanning with a very high pitch (>3) on a dual-source scanner allowing to scan the entire heart in around 250 ms.⁹

The timing of contrast media administration can be performed via the bolus-tracking or the test-bolus injection technique, depending on institutional preferences to optimize the contrast opacification of the anatomy of interest. To image cardiac venous anatomy, typically 2–4 s are added to the conventional post-trigger delay applied in coronary CT angiography.^{10,11}

CT images for treatment planning are acquired from the carina to the diaphragm in a single-breath hold. Isotropic submillimeter voxels then allow for multiplanar reformations and 3D reconstructions. Iterative reconstruction algorithms enable the reduction of image noise having also the potential to reduce radiation doses while preserving an adequate contrast-to-noise level.¹²

A delayed phase imaging of the LAA improves the diagnostic accuracy to rule-out thrombus, as filling defects of the stunned left atrial appendage in first pass angiography may simulate thrombus¹³ (Figure 1). Interestingly, the literature about timing of the delayed-phase scan is heterogenous ranging between a delay of 40 s¹⁴ to a delay of 6 min after the acquisition of the initial scan.¹⁵ Spagnolo et al¹⁵ showed that a 6 min delay may further improve the diagnostic accuracy of thrombus detection compared to a delay of 1 min or 3 min after contrast administration. Spectral CT with material decomposition may assist in correctly depicting thrombi through iodine concentration quantification.¹⁶

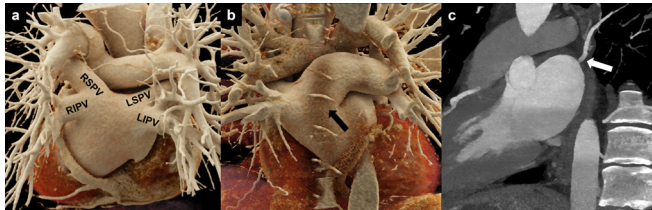
When it is intended to detect myocardial fibrosis and scar with CT, a delayed scan for iodine late enhancement imaging must be performed at the equilibrium phase of contrast media distribution around 5 min after intravenous injection.^{17–19} Left ventricular extracellular volume fraction as a measure of myocardial fibrosis shows a strong correlation between CT and the reference standard MRI.²⁰

Anatomy of the LA and PV

Assessing the anatomy of the left atrium (LA) and pulmonary veins (PVs) is crucial for pre-procedural planning of patients with AF.²¹ The LA is the most posterior cardiac chamber and comprises several components: the vestibule (the portion surrounding the mitral valve), the LAA, the septum (in common with the right atrium), the anterior wall (inferior to the Bachmann's bundle), which is the thinnest part of the LA (1.5–4.8 mm), and the dome, which is the thickest part (3.5–6.5 mm).²² Within the septal wall, the foramen ovale can be identified as a bilaminar valve of fibrous tissue, delimited by a muscular rim.²³ The posterior wall of the LA that is included among PV inflow vestibula is referred to as the "posterior LA".²¹ The intervenous saddle is the LA portion between two ipsilateral PVs, and, together with PV ostia, forms the PV inflow vestibule. The PV trunk represents the portion of the PV vessel between the ostia and the first branch.²⁴

In normal PV anatomy (which accounts for almost the 70% of the general population²⁴), four separate ostia can be found. Two from the right side: the superior right vein (RSPV), draining the upper and middle pulmonary lobe, and the inferior right vein (RIPV) draining the inferior pulmonary lobe. And two from the left side: the superior left vein (LSPV), draining the upper pulmonary lobe, and the inferior left vein (LIPV), for the inferior pulmonary lobe²¹ (Figure 2a). The most frequent PV variants include the so-called "conjoined vein" (2–25% of the population), which is defined as joining of the superior and inferior PV draining into the LA with a common ostium (most often involving the left PVs)^{25–27} (Figure 2b). Other variants include the presence of accessory veins: the most common are the right middle vein

Figure 2. PV anatomy. (a) Cinematic 3D rendering of the heart showing the posterior aspect of the LA with normal PV anatomy: two veins to the right (RSPV and RIPV) and two veins to the left (LSPV and LIPV) joining the LA. (b) Cinematic 3D rendering showing a single PV ostium for the superior and inferior left pulmonary veins (conjoined vein, black arrow). (c) white arrow highlighting an accessory pulmonary vein (right top vein). LA, left atrium; LIPV, left inferior pulmonary vein; LSPV, left superior pulmonary vein; RIPV, right inferior pulmonary vein; RSPV, right superior pulmonary vein; PV, pulmonary vein.



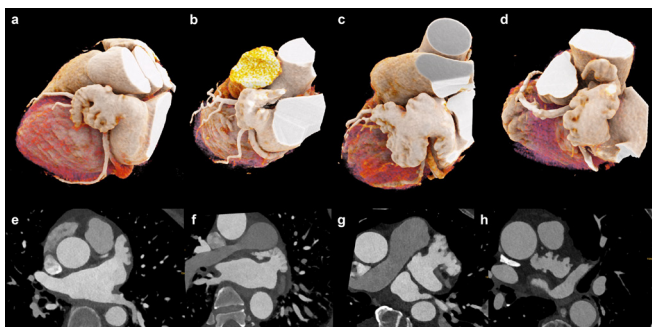
(incidence of 9–26.6%), the right top vein (0.3–9.3%) (Figure 2c) and the left middle vein (0.1–0.5%)²¹; and the early branching of the PV in which the PV trunk is shorter than 5 mm.²¹

Anatomy of the LAA

The LAA is an embryonic remnant extension of the LA containing trabeculations from pectinate muscles that cover its endocardial surface.²⁸ An LAA lobe is defined as an extroversion of the LAA wall with a minimum depth and width of 1 cm. According to its shape, four different morphologies have been identified²⁹: the “chicken wing” type with a sharp bend in the proximal or middle aspect of the dominant lobe; the “windsock” type with a dominant lobe and multiple secondary lobes in the inferior direction; the “cactus” type with a central primary lobe and multiple secondary lobes, developing both in superior and inferior directions and the “cauliflower” type, with no dominant lobe and an irregular shape of the orifice³⁰ (Figure 3).

According to Wang et al,³⁰ several orifice shapes of the LAA exist: oval in 69%, foot-like in 10%, triangular in 8%, water-drop like in 8%, and round in 6%. Based on the relationship between the superior and the inferior aspect of the LAA and the LSPV and

Figure 3. Types of left atrial appendage configuration. Cinematic 3D rendering (a–d) and multiplanar reformations (e–h) of left atrial appendage morphology types. (a, e) Windsock variant. (b, f) Chicken-wing variant. (c, g) Cauliflower variant. (d, h) Cactus variant.



LIPV, a high, mid, and low LAA take-off can be distinguished.²⁹ If the superior wall of the LAA is located at the same height as compared to the superior aspect of the LSPV, the take-off is “high”; if it is found between the LSPV and LIPV ostium it is considered “mid”; and when located inferiorly to the inferior wall of the LSPV it is referred to as “low”.²⁹

Coronary vein anatomy

When planning cardiac resynchronization therapy, it is important to recognize cardiac veins and their anatomic variants. The epicardial veins (great cardiac venous system) drain 70% of the cardiac venous blood.³¹ Approximately, two-thirds of the epicardial veins finally drain into the great cardiac vein or in the CS.³¹ The CS is the continuation of the great cardiac vein running in the left atrioventricular sulcus. Its ostium in the right atrium (posteroseptal wall) is often delimited by the Thebesian valve.³² The anterior interventricular vein runs in the interventricular groove towards the cardiac base, where it turns into the great cardiac vein. The other great cardiac venous system veins are located between the posterior wall of the left ventricle and the anterior interventricular vein and are characterized by several variants in numbers and caliber. Those are the middle cardiac vein, which runs in the posterior interventricular groove and joins the CS; the left marginal vein, found in 70–95% of the individuals and draining in the great cardiac vein in the 80%; the posterolateral vein (single vein in 60% of the subjects, usually draining in the CS), the lateral vein (present in almost the 80% of patients), the anterolateral vein and the anterior vein^{31,32} (Figure 4).

The oblique vein of the left atrium, also called the Marshall vein, is an embryonic remnant of the left superior vena cava. The pericardial fold around this vessel may be a source of paroxysmal AF. The Marshall vein joins the great coronary vein at the level of the valve of Vieussens,³² located at the junction between the great cardiac vein and the CS.¹¹

Pre-procedural imaging

Coronary artery disease

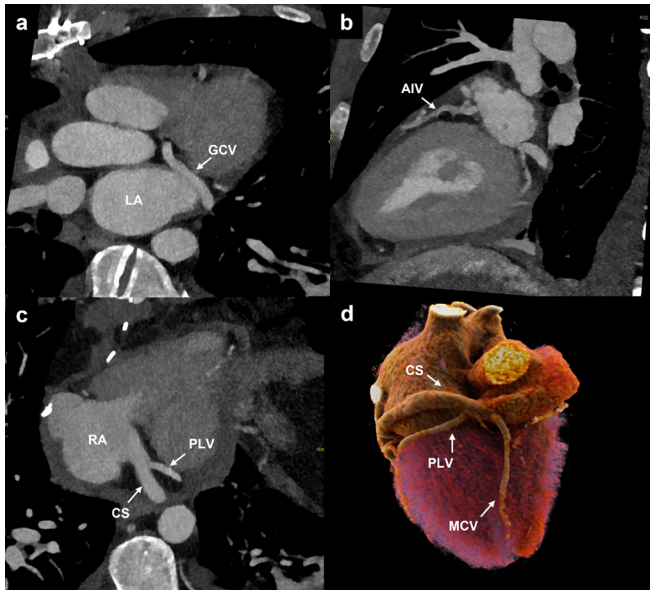
Coronary artery disease may be a substrate for AF³³ and both diseases share common risk factors including smoking, diabetes, and arterial hypertension.³³ In pre-procedural cardiac CT, coronary artery assessment can be performed alongside with the evaluation of the cardiac anatomy. For this reason, the administration of 400–800 µg of sublingual nitroglycerine is recommended³⁴ prior to cardiac CT and care should be taken for heart rate control in order to acquire images without motion artifacts of the coronaries. Patients with AF benefit from imaging with high temporal resolution as discussed above.³⁵

In patients with ventricular arrhythmia and a low-pretest probability of coronary artery disease, coronary CT may be used to rule-out relevant coronary artery stenosis and coronary artery anomalies as a substrate for ventricular arrhythmia.²

Pulmonary vein isolation

AF is the most common cardiac arrhythmia with an estimated prevalence of 2–4%.³⁶ The prevalence is expected to rise due to

Figure 4. Cardiac vein anatomy. (a) Oblique axial reformation showing the GCV running in the atrioventricular sulcus. (b) Oblique sagittal reformation illustrating the anterior interventricular vein, which runs in the anterior interventricular sulcus from the apex towards the base of the heart. (c) Oblique axial reformation demonstrating the CS draining into the RA after receiving the PLV. (d) Cinematic 3D rendering showing the posterior aspect of the heart with the MCV running in the posterior interventricular sulcus and draining directly into the RA. CS and PLV are also represented. CS, coronary sinus; GCV, great cardiac vein; MCV, middle cardiac vein; LA, left atrium; PLV, posterolateral vein; RA, right atrium.



the continuous aging of the general population and the intensified search for the disease.^{37,38} AF is associated with an increased risk of thromboembolic disease and heart failure as well as an increased risk of all-cause mortality.³⁶

A thin myocardial layer around the pulmonary veins is a major source of ectopic atrial beats.³⁹ The goal of catheter ablation is to electronically isolate the ectopic foci accessing the left atrium via a transeptal approach.³⁹ However, persistent electrical isolation of the pulmonary veins is difficult to achieve with reported reconnection rates of more than 70%.⁴⁰ Therefore, supplementary ablation lines are recommended in patients with long-standing AF, including extrapulmonary areas such as the LAA, the superior vena cava or in low-voltage areas.⁴¹

Pulmonary vein isolation is effective in patients with paroxysmal and persistent AF.³⁹ Blomstrom-Lundqvist et al have shown that patients undergoing catheter ablation have a better quality of life compared to patients undergoing medical therapy alone.⁴² However, catheter ablation may not improve the rates of death, cardiac arrest, disabling stroke or serious bleeding compared to medical therapy.⁴³

Pre-procedural CT is valuable for evaluating the anatomy and dimensions of the LA, for ruling-out thrombus, and for assessing the number and anatomical configuration of pulmonary veins.

This information may assist the operator in choosing the right catheter, in positioning the catheter during the procedure, and to plan the most appropriate ablation strategy.

Furthermore, CT provides information on the course of the esophagus, anatomy of the superior and inferior vena cava as well as the location of the fossa ovalis. The presence of lipomatous hypertrophy of the atrial septum may interfere with transeptal puncture.

Pre-procedural CT images may also be used for image fusion with electroanatomical maps and real-time fluoroscopic images with the potential to reduce procedure times and fluoroscopic radiation exposure.⁴⁴

LAA occlusion—indications and patient benefit

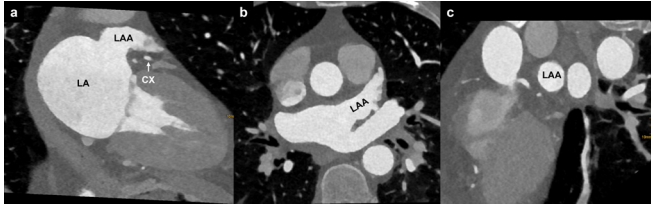
The LAA is responsible for almost 90% of cardiac thrombi in patients with non-valvular associated AF. Therefore, LAA occlusion represents a therapeutic option for treating patients with AF, especially in those who show recurrent emboli or contraindication to therapy with anticoagulants (elevated bleeding risk, non-compliant patients).¹⁰ Several techniques of LAA exclusion exist, both surgical and percutaneous. The formers include epicardial or endocardial ligation or clipping of the LAA ostium,⁴⁵ surgical excision of the LAA or the device-enabled occlusion method.⁴⁶ As less-invasive methods, endovascular approaches can be adopted: the plug system in which the device obstructs the LAA at the level of the orifice; the pacifier system, where the lobe of the device is associated to a disc that faces the LA lumen and closes the LAA; and the ligation technique that allows closure of the LAA neck with an endocardial–epicardial approach.²⁸ Despite the lack of clinical data and randomized controlled trials, surgical LAA occlusion/excision is recommended in case of open-heart surgery, whereas transcatheter LAA occlusion is predominantly indicated in subjects with high risk of stroke and contraindications to anticoagulants.⁴⁷

Size, morphology of the LAA, position of the ostia, and where to measure

Pre-procedural evaluation of patients undergoing LAA occlusion can be performed both with transesophageal echocardiography (TEE) and with CT.²⁸ First, the presence of a thrombus in the lumen of LAA must be ruled out, as this condition represents a contraindication to the procedure. TEE is still considered the reference standard, but cardiac CT is gaining increasing importance thanks to its high diagnostic accuracy when a delayed contrast phase is acquired (sensitivity 98%, specificity 100%).⁴⁸ CT may also assist in unclear TEE cases to distinguish between spontaneous echocardiographic contrast associated with slow blood flow and true thrombus.⁴⁹

TEE is a valid and robust technique that allows LAA evaluation with a good anatomic definition, analyzing maximum and minimum LAA diameters in end-systole. On the other hand, cardiac CT allows for 3D measurements and multiplanar reformations for a better definition of LAA orifice diameters, morphology, length, angulation and lobes, the relationship between its superior and inferior aspects and the LPVs, and

Figure 5. Evaluation of LAA anatomy prior to the before occlusion procedure. (a) Oblique sagittal LAA reformation (both long axis LAA and circumflex artery are visualized). (b) Orthogonal plane (axial to the LAA walls). (c) Oblique plane to evaluate the LAA orifice. CX: circumflex artery; LA, left atrium; LAA, left atrial appendage.



the atrial landing zone⁴⁹ (distance between mitral annulus or circumflex artery and the LSPV vestibulum).⁴⁹

When using cardiac CT, it is important to evaluate the LAA in the end-systolic phase (30–40% of the cardiac cycle) to assess the greatest dimensions of the LAA.⁵⁰ Fundamental reformations are: (1) the oblique LAA view (circumflex artery and long-axis LAA should be visualized); (2) an orthogonal plane of this section in order to be axial to the LAA walls; (3) a double oblique plane to evaluate the ostium diameters (Figure 5). According to the literature, cardiac CT gives more precise measurements as compared to TEE and fluoroscopy.^{51–53} Based on several studies,^{52–54} cardiac CT provides larger measurements as compared to TEE (1–3 mm greater, both for 2D and for 3D techniques) and fluoroscopy (2–4 mm greater), thanks to 3D and multiplanar reformations which allow for the evaluation of the maximal dimensions. Cardiac CT also helps selecting the fluoroscopic angles for the transcatheter procedure. Necessary measurements could vary according to the type of device that is used.

ICD and CRT implantation

ICD implantation is an integral part of treatment of patients with sustained cardiac arrest due to ventricular arrhythmia or with an increased risk of sudden cardiac death.^{2,55} CRT implantation reduces mortality in heart failure⁵⁵ in patients with mechanical dyssynchrony.

In CRT and ICD patients, CT venography may provide important information on the patency of the subclavian veins and superior vena cava, especially in patients with previous clavicular fractures or patients scheduled for CRT or ICD replacement. 3D, non-invasive assessment of the cardiac venous anatomy may assist treatment planning as the cardiac venous anatomy is highly variable.¹¹ Interventional lead placement can be facilitated by providing information on the presence of a prominent or calcified Thebesian valve, on size, angle and location of the coronary sinus and the position and branching of the coronary veins. To achieve resynchronization of the left ventricle with a CRT-device, it is critical that the LV lead is positioned in the area of delayed electrical activation and mechanical contraction.⁵⁶ Sommer et al compared clinical outcomes between patients who underwent CT venography and SPECT myocardial perfusion assessment and those who underwent no imaging prior to CRT and demonstrated that the imaging-guided strategy reduced the

rate of non-response to CRT.⁵⁷ Therefore, even if fluoroscopy venography assessment is performed during the CRT procedure, a prior evaluation of the anatomy with cardiac CT has the potential to improve response to treatment. Similarly, a recent meta-analysis revealed that multimodality imaging improves left ventricular end-systolic volume and the general response to CRT as compared to fluoroscopic guidance alone.⁵⁸

The standard of reference for myocardial fibrosis assessment and quantification is CMR. However, there are some limitations of the technique: patients with claustrophobia or with metal implants often cannot be scanned with CMR, the downside of a long acquisition time, and the required expertise.⁵⁹ CT can assess the presence of myocardial scar either by visualization of left myocardial wall thinning and lipomatous metaplasia or by the detection of delayed iodine enhancement and increased ECV on dedicated late iodine enhancement scans relatively easily.^{17,18} (Figure 6), with faster acquisition time, larger accessibility, less expensive, and with comparable diagnostic accuracy.⁶⁰ Furthermore, 4DCT with acquisition of image data throughout the cardiac cycle may help visualizing mechanical dyssynchrony. Buss et al showed that CT has a higher reproducibility and faster analysis time for diagnosing mechanical dyssynchrony of the ventricles compared to real-time 3D echocardiography.⁶¹ CT measurements of dyssynchrony are based on myocardial wall thickness (epicardial and endocardial borders) changes over the cardiac cycle, rather than the 3D-echocardiographic method which only takes into account the endocardial contour. Despite the lower temporal resolution of CT, which is reduced with dual source scanners, CT assessments are associated with a greater reproducibility and faster imaging time than echocardiography.⁶²

Ventricular tachycardia

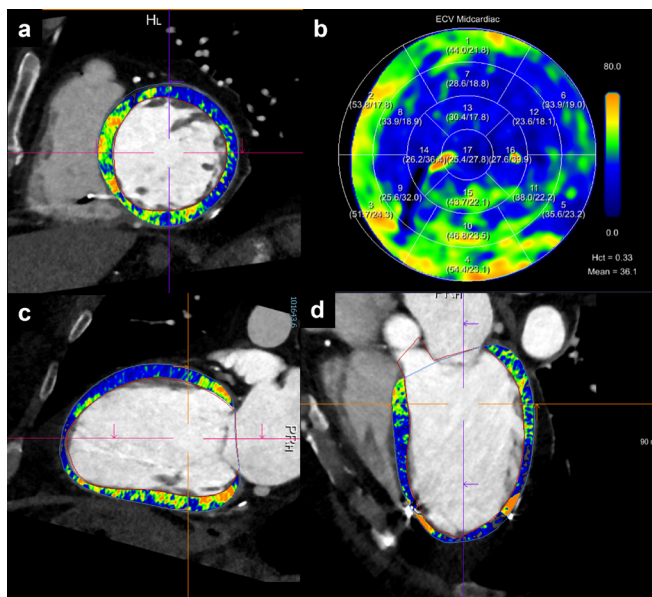
Given the high correlation between myocardial scarred segments and regions of low bipolar voltages at electroanatomic mapping,⁶³ the identification of regions of reduced wall thickness⁶⁴ or late iodine enhancement⁶³ with dedicated CT late iodine enhancement scans,^{17,18} is specifically useful prior to ventricular tachycardia ablation procedures. In this scenario, CT has the potential to depict fibrotic myocardial areas in patients with contraindications for cardiac MR imaging. Moreover, CT assessment of epicardial fat improves the evaluation of epicardial voltage maps and epicardial fat thickness,⁶⁵ which may be of importance in electrophysiological procedures.

Post-procedural imaging

Imaging of complications

As suggested by the 2020 EHRA/EAPCI expert consensus statement,²⁸ follow-up imaging of patients after LAA occlusion is recommended 6–12 weeks after device implantation, both with TEE and CCT⁶³ and shall be repeated after 12 months in patients with thromboembolic events.⁶⁴ Besides the value of CT for routine follow-up imaging after LAA occlusion, CT is also the primary modality for the detection of procedure-related complications, which occur in around 5% of the interventions.^{24,65,66} Some changes of cardiac structures are often encountered after catheter-based radiofrequency ablation, such as a LA scar along the ablation line and an inverse remodeling of the atrial chamber

Figure 6. Scar detection. A 60-year-old female patient with ischemic cardiomyopathy, reduced ejection fraction and ICD implantation. Ablation was planned due to an episode of ventricular tachycardia with cardiogenic shock. Cardiac photon-counting detector CT with acquisition of a dual-energy late enhancement phase (after 5 min.) revealed an extensive post-ischemic scar in anterior and anteroseptal segments of the basal and mid-ventricular left ventricle (**a, c, d**), with associated increased extracellular volume fraction (**b**). Successful radiofrequency ablation confirmed left ventricular tachycardia associated with the scar, with mid-diastolic potentials in anteroseptal, anterior and anterolateral segments from basal to midventricular planes. ICD, implantable cardioverter defibrillator



with reduction in LA volume and increased contractility.⁶⁷ Critical and non-intended complications include pulmonary vein stenosis or occlusion, acute pulmonary injury, mitral valve injury, tamponade, hemothorax, atrioesophageal fistula, and stroke. Most of these complications occur within 24 h after the procedure but may also appear after 1–2 months.⁶⁸

PV stenosis has an incidence of 0.29% after catheter-based radiofrequency ablation,¹⁰ is often asymptomatic and can lead

Figure 7. PV stenosis after radiofrequency catheter ablation. (**a**) PV ostium before procedure. (**b**) Ostium wall thickening with PV stenosis after RFCA (black arrows). PV, pulmonary vein; RFCA, radiofrequency catheter ablation.

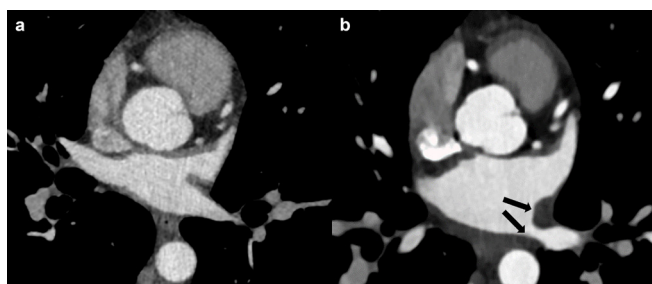
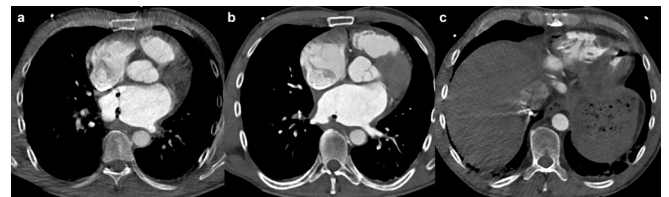


Figure 8. Atrioesophageal fistula after radiofrequency catheter ablation. Air bubbles and thrombus inside the left atrium (**a, b**) and the left ventricle (**c**).



to pulmonary infarction and pulmonary hypertension.^{10,24} The degree of stenosis can be easily evaluated with cardiac CT and is classified as severe (>70%), moderate (50–69%), and mild (<50%)⁶⁶ (Figure 7).

Atrioesophageal fistula is a rare and fatal complication with an incidence of 0.04%⁶⁹ that is associated with catheter-based radiofrequency ablation procedures on the posterior LA wall, given the proximity between the esophagus and the LSPV and LIPV (10)(67). CT represents the imaging technique of choice, showing air bubbles in the mediastinum and stranding of the mediastinal fat¹⁰ or in more severe cases, thrombus formation in the left atrium and air in the heart (Figure 8). Further potentially life-threatening complications of catheter-based radiofrequency ablation are periprocedural thromboembolic events and cardiac tamponade, both with a complication rate of around 1%.⁷⁰

Patency assessment after LAA occlusion

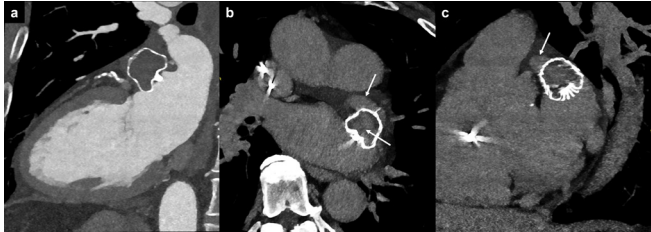
Imaging after LAA occlusion is performed to determine the success of the procedure. Patency assessment can be done quantitatively (e.g. defined as an attenuation in the LAA distal to the device of above 100 HU in the arterial phase⁷¹ and/or qualitatively, defined as visual contrast media pooling in the LAA distal to the device in the arterial and/or later phases).

LAA patency rates are variable as they depend on the implanted device, on the timing of imaging after the procedure, and on the modality for imaging. While TEE is often used as the first-line imaging modality for the surveillance of LAA patency, it is known to have a limited sensitivity compared to cardiac CT, the latter representing the most accurate imaging tool for LAA assessment after intervention.⁶³

When using TEE, patency rates with the Watchman device range from 0.2% when considering only leaks >5 mm⁷² to 32.1% at 1-year follow-up including all kinds of peridevice flow.⁷³ In distinction, patency rate when assessed by cardiac CT performed after an average of 142 days after LAA occlusion⁷¹ using the Amplatzer plug, the Watchman and the Amplatzer Amulet were 70.6%, 55.6%, and 66.7%, respectively. Jaguszewski et al¹⁴ showed residual patency over a 3 months follow-up after LAA occlusion with an Amplatzer plug in 62% of patients as assessed by cardiac CT with all leaks being <4 mm, whereas TEE only detected patency in 36%.

When LAA patency after intended occlusion is detected the underlying mechanism should be determined as follows⁶³: (i)

Figure 9. Fabric permeability. LAA patency after Watchman device implantation. (a) The arterial phase CT indicates apparent complete occlusion of the LAA. (b, c) The very delayed phase (5min) reveals increased attenuation in the LAA and within the device itself (white arrows), suggestive for LAA patency due to fabric permeability. LAA, left atrial appendage.



fabric permeability, defined as device permeability observed by passage of the contrast through the non-endothelialized membrane despite appropriate proximal device apposition⁷⁴ (Figure 9); (ii) malapposition of the proximal segment of the device lobe, in which contrast is present in any of the proximal quadrants (not fulfilling the peridevice leak criteria below) enabling communication between the LA and the distal LAA through the lobe (Figure 10); and (iii) peridevice leak, defined as a contrast opacification all along the lobe perimeter allowing communication between the LA and the distal LAA⁷⁵ (Figure 11).

It is important to know that TEE is not able to detect malpositioning of the device as well as fabric permeability,⁶³ thus limiting the usefulness of this modality in clinical routine. Malapposition of the proximal segment of the device lobe is the most observed mechanism for LAA patency and is typically (70–80%) located at the posteroinferior quadrant.

While patency can be readily detected with cardiac CT (and to a lesser extent with TEE), its clinical relevance remains a matter of continuing debate. The current believe is that patency, when the gap is smaller than 3 mm in diameter, is not associated with adverse events. Korsholm et al⁷⁶ reported that a peridevice leak was found with cardiac CT in 61% of the patients after LAA occlusion, but the existence of a peridevice leak was not associated with clinical outcome (composite of ischemic stroke, transient ischemic attack, systemic embolism, or all-cause death) after a median follow-up duration of

Figure 10. Malapposition of device for left atrial appendage occlusion. Malposition of the proximal segment of the device lobe in axial (a), oblique coronal (b), and oblique axial (c) reformations, with persistent opacification of the left atrial appendage via the posterior quadrant (red curved arrow).

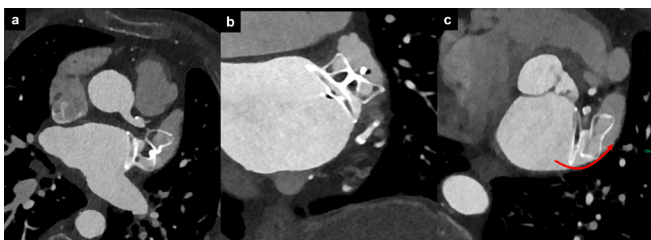
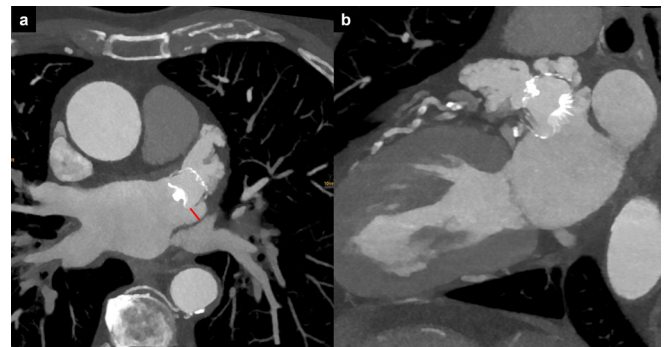


Figure 11. Peridevice leak. (a) Axial and (b) oblique sagittal reformation of the LAA showing its complete opacification after LAA occlusion with the Watchman device, due to a peridevice leak (>5 mm, red line). LAA, left atrial appendage



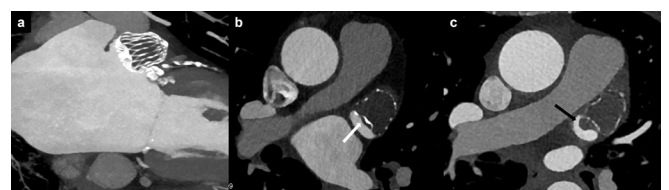
2.6 years. Agudelo et al⁶³ found that LAA patency as detected with cardiac CT was frequent (57%) but not associated with adverse outcomes (defined as an increase in mortality, cerebrovascular accident or bleeding events) at a median follow-up of 608 days.

Device-related thrombus

Device-related thrombus (DRT) is another potentially relevant complication occurring after LAA occlusion, with a reported prevalence between 1.5 and 4.2%.^{77–79} Similar to LAA patency, the prevalence of DRT depends on the modality used for follow-up and on the timing of imaging after the procedure.⁸⁰ When detected, DRT is usually classified into low-grade hypoattenuated thickening (HAT) with <3 mm of thickness and a laminar shape, and into high-grade HAT with >3 mm and irregular or pedunculated thickening at the atrial side of the device⁸¹ (Figure 12). While low-grade HAT has been rather related to a “physiological” endothelialization process on the device surface favored by complete LAA occlusion and with no relation with adverse events, high-grade HAT has been associated with a three- to fivefold increase in stroke and systemic embolization.⁶³

While DRT can be readily detected with CT, its therapeutic consequences remain a matter of debate and treatment recommendations vary.⁸⁰ While anticoagulation is effective in resolving DRT in the majority of patients, concerns remain about the optimal candidates for resuming anticoagulation,

Figure 12. Device-related thrombus. (a) Normal LAA occluder position; (b) low-grade HAT (<3mm, white arrow); (c) high grade HAT (>3mm, black arrow). HAT, hypoattenuated thickening; LAA, left atrial appendage



the duration of medication, and the risk of recurrence of DRT upon cessation of anticoagulation.

CONCLUSION

CT plays an increasingly important role in the pre-interventional but also in post-interventional evaluation of patients with arrhythmia. Besides the evaluation of coronary artery disease, cardiac CT may add valuable information before occlusion of the LAA, PV isolation, and cardiac device implantation as well as for the rapid evaluation of periprocedural complications. In addition, cardiac CT is increasingly used as a non-invasive and

accurate tool for the post-procedural surveillance of patients with arrhythmia.

FUNDING

G.C. received a grant from the European School of Radiology (ESOR) to finance the Scholarship Training Programme. Open access funding provided by Universitat Zurich.

DISCLOSURE

H.A.: Institutional grants from Bayer, Canon, Guerbet, Siemens
H.A.: Speaker's bureau Siemens.

REFERENCES

- Hindricks G, Potpara T, Dagres N, Arbelo E, Bax JJ, Blomström-Lundqvist C. 2020 ESC guidelines for the diagnosis and management of atrial fibrillation developed in collaboration with the European Association for Cardio-Thoracic surgery (EACTS). *Eur Heart J* 2021; **42**: 373–498. Available from: <https://academic.oup.com/eurheartj/article/42/5/373/5899003>
- Zeppenfeld K, Tfelt-Hansen J, de Riva M, Winkel BG, Behr ER, Blom NA, et al. 2022 ESC guidelines for the management of patients with ventricular arrhythmias and the prevention of sudden cardiac death. *Eur Heart J* 2022; **43**: 3997–4126. <https://doi.org/10.1093/eurheartj/ehac262>
- Hell MM, Achenbach S. CT support of cardiac structural interventions. *Br J Radiol* 2019; **92**(1098): 20180707. <https://doi.org/10.1259/bjr.20180707>
- Lewis MA, Pascoal A, Keevil SF, Lewis CA. Selecting a CT scanner for cardiac imaging: The heart of the matter. *Br J Radiol* 2016; **89**(1065): 20160376. <https://doi.org/10.1259/bjr.20160376>
- Clayton B, Roobottom C, Morgan-Hughes G. CT coronary angiography in atrial fibrillation: A comparison of radiation dose and diagnostic confidence with retrospective gating vs prospective gating with systolic acquisition. *Br J Radiol* 2015; **88**(1055): 20150533. <https://doi.org/10.1259/bjr.20150533>
- Korsholm K, Samaras A, Andersen A, Jensen JM, Nielsen-Kudsk JE. The Watchman FLX device. *JACC: Clinical Electrophysiology* 2020; **6**: 1633–42. <https://doi.org/10.1016/j.jacep.2020.06.028>
- Alkadhhi H, Leschka S. Radiation dose of cardiac computed tomography – what has been achieved and what needs to be done. *Eur Radiol* 2011; **21**: 505–9. <https://doi.org/10.1007/s00330-010-1984-3>
- Euler A, Higashigaito K, Mergen V, Sartoretti T, Zanini B, Schmidt B, et al. High-pitch photon-counting detector computed tomography angiography of the aorta. *Invest Radiol* 2022; **57**: 115–21. <https://doi.org/10.1097/RLI.0000000000000816>
- Achenbach S, Marwan M, Schepis T, Pflederer T, Bruder H, Allmendinger T, et al. High-pitch spiral acquisition: A new Scan mode for coronary CT angiography. *J Cardiovasc Comput Tomogr* 2009; **3**: 117–21. <https://doi.org/10.1016/j.jcct.2009.02.008>
- Liddy S, Buckley U, Kok HK, Loo B, Glover B, Dhillon GR, et al. Applications of cardiac computed tomography in electrophysiology intervention. *Eur Heart J Cardiovasc Imaging* 2018; **19**: 253–61. <https://doi.org/10.1093/ehjci/jex312>
- Sirajuddin A, Chen MY, White CS, Arai AE. Coronary venous anatomy and anomalies. *J Cardiovasc Comput Tomogr* 2020; **14**: 80–86. <https://doi.org/10.1016/j.jcct.2019.08.006>
- Gordic S, Desbiolles L, Sedlmair M, Manka R, Plass A, Schmidt B, et al. Optimizing radiation dose by using advanced modelled iterative reconstruction in high-pitch coronary CT angiography. *Eur Radiol* 2016; **26**: 459–68. <https://doi.org/10.1007/s00330-015-3862-5>
- Hur J, Kim YJ, Lee H-J, Ha J-W, Heo JH, Choi E-Y, et al. Left atrial Appendage thrombi in stroke patients: Detection with two-phase cardiac CT angiography versus Transesophageal echocardiography. *Radiology* 2009; **251**: 683–90. <https://doi.org/10.1148/radiol.2513090794>
- Jaguszewski M, Manes C, Puipe G, Salzberg S, Müller M, Falk V, et al. Cardiac CT and Echocardiographic evaluation of peri-device flow after percutaneous left atrial Appendage closure using the AMPLATZER cardiac plug device. *Catheter Cardiovasc Interv* 2015; **85**: 306–12. <https://doi.org/10.1002/ccd.25667>
- Spagnolo P, Giglio M, Di Marco D, Cannà PM, Agricola E, Della Bella PE, et al. Diagnosis of left atrial Appendage thrombus in patients with atrial fibrillation: Delayed contrast-enhanced cardiac CT. *Eur Radiol* 2021; **31**: 1236–44. <https://doi.org/10.1007/s00330-020-07172-2>
- Hur J, Kim YJ, Lee H-J, Nam JE, Hong YJ, Kim HY, et al. Cardioembolic stroke: Dual-energy cardiac CT for differentiation of left atrial Appendage thrombus and circulatory stasis. *Radiology* 2012; **263**: 688–95. <https://doi.org/10.1148/radiol.12111691>
- Mergen V, Sartoretti T, Klotz E, Schmidt B, Jungblut L, Higashigaito K, et al. Extracellular volume Quantification with cardiac late enhancement scanning using dual-source photon-counting detector CT. *Invest Radiol* 2022; **57**: 406–11. <https://doi.org/10.1097/RLI.0000000000000851>
- Scully PR, Patel KP, Klotz E, Augusto JB, Thornton GD, Saberwal B, et al. Myocardial fibrosis quantified by cardiac CT predicts outcome in severe aortic stenosis after transcatheter intervention. *JACC Cardiovasc Imaging* 2022; **15**: 542–44. <https://doi.org/10.1016/j.jcmg.2021.10.016>
- van Assen M, De Cecco CN, Sahbae P, Eid MH, Griffith LP, Bauer MJ, et al. Feasibility of extracellular volume quantification using dual-energy CT. *Journal of Cardiovascular Computed Tomography* 2019; **13**: 81–84. <https://doi.org/10.1016/j.jcct.2018.10.011>
- Ohta Y, Kishimoto J, Kitao S, Yunaga H, Mukai-Yatagai N, Fujii S, et al. Investigation of myocardial extracellular volume fraction in heart failure patients using iodine map with rapid-kV switching dual-energy CT: Segmental comparison with MRI T1 mapping. *J Cardiovasc Comput Tomogr* 2020; **14**: 349–55. <https://doi.org/10.1016/j.jcct.2019.12.032>
- Pandey NN, Taxak A, Kumar S. Normal pulmonary venous anatomy and non-

- anomalous variations demonstrated on CT angiography: What the radiologist needs to know? *BJR* 2020; **93**: 20200595. <https://doi.org/10.1259/bjr.20200595>
22. Whiteman S, Saker E, Courant V, Salandy S, Gielecki J, Zurada A, et al. An anatomical review of the left atrium. *Translational Research in Anatomy* 2019; **17**: 100052. <https://doi.org/10.1016/j.tria.2019.100052>
 23. Ho SY, McCarthy KP. Anatomy of the left atrium for interventional electrophysiologists. [Internet]. *Pacing Clin Electrophysiol* 2010; **33**: 620–27. <https://doi.org/10.1111/j.1540-8159.2009.02659.x>
 24. Niinuma H, George RT, Arbab-Zadeh A, Lima JAC, Henrikson CA. Imaging of pulmonary veins during catheter ablation for atrial fibrillation: the role of multi-slice computed tomography. *Europace* 2008; **10** Suppl 3: iii14–21. <https://doi.org/10.1093/europace/eun230>
 25. Marom EM, Herndon JE, Kim YH, McAdams HP. Variations in pulmonary venous drainage to the left atrium: Implications for radiofrequency ablation. *Radiology* 2004; **230**: 824–29. <https://doi.org/10.1148/radiol.2303030315>
 26. Scharf C, Sneider M, Case I, Chugh A, Lai SWK, Pelosi F, et al. Anatomy of the pulmonary veins in patients with atrial fibrillation and effects of segmental Ostial ablation analyzed by computed tomography. *J Cardiovasc Electrophysiol* 2003; **14**: 150–55. <https://doi.org/10.1046/j.1540-8167.2003.02444.x>
 27. Cronin P, Sneider MB, Kazerooni EA, Kelly AM, Scharf C, Oral H, et al. MDCT of the left Atrium and pulmonary veins in planning radiofrequency ablation for atrial fibrillation: A how-to guide. *AJR Am J Roentgenol* 2004; **183**: 767–78. <https://doi.org/10.2214/ajr.183.3.1830767>
 28. Glikson M, Wolff R, Hindricks G, Mandrola J, Camm AJ, Lip GYH, et al. EHRA/EAPCI expert consensus statement on catheter-based left atrial Appendage occlusion – an update. *Europace* 2020; **22**: 184. <https://doi.org/10.1093/europace/euz258>
 29. Budge LP, Shaffer KM, Moorman JR, Lake DE, Ferguson JD, Mangrum JM. Analysis of in vivo left atrial Appendage morphology in patients with atrial fibrillation: a direct comparison of Transesophageal echocardiography, planar cardiac CT, and Segmented three-dimensional cardiac CT. *J Interv Card Electrophysiol* 2008; **23**: 87–93. <https://doi.org/10.1007/s10840-008-9281-7>
 30. Wang Y, Di Biase L, Horton RP, Nguyen T, Morhanty P, Natale A. Left atrial appendage studied by computed tomography to help planning for appendage closure device placement. *J Cardiovasc Electrophysiol* 2010; **21**: 973–82. <https://doi.org/10.1111/j.1540-8167.2010.01814.x>
 31. Saremi F, Muresian H, Sánchez-Quintana D. Coronary veins: Comprehensive CT-anatomic classification and review of variants and clinical implications. *Radiographics* 2012; **32**: E1–32. <https://doi.org/10.1148/rg.321115014>
 32. Mlynarski R, Mlynarska A, Sosnowski M. Anatomical variants of coronary venous system on cardiac computed tomography. *Circ J* 2011; **75**: 613–18. <https://doi.org/10.1253/circj.cj-10-0736>
 33. Nishida K, Qi XY, Wakili R, Comtois P, Chartier D, Harada M, et al. Mechanisms of atrial tachyarrhythmias associated with coronary artery occlusion in a chronic canine model. *Circulation* 2011; **123**: 137–46. <https://doi.org/10.1161/CIRCULATIONAHA.110.972778>
 34. Abbara S, Blanke P, Maroules CD, Cheezum M, Choi AD, Han BK, et al. SCCT guidelines for the performance and acquisition of coronary computed Tomographic angiography: A report of the society of cardiovascular computed tomography guidelines committee. *J Cardiovasc Comput Tomogr* 2016; **10**: 435–49. <https://doi.org/10.1016/j.jcct.2016.10.002>
 35. Sun G, Li M, Jiang Z, Xu L, Peng Z, Ding J, et al. Diagnostic accuracy of dual-source CT coronary angiography in patients with atrial fibrillation: Meta analysis. *Eur J Radiol* 2013; **82**: 1749–54. <https://doi.org/10.1016/j.ejrad.2013.04.034>
 36. Benjamin EJ, Muntner P, Alonso A, Bittencourt MS, Callaway CW, Carson AP, et al. Heart disease and stroke Statistics—2019 update: A report from the American heart Association. *Circulation* 2019; **139**: e56–528. <https://doi.org/10.1161/CIR.0000000000000659>
 37. Krijthe BP, Kunst A, Benjamin EJ, Lip GYH, Franco OH, Hofman A, et al. Projections on the number of individuals with atrial fibrillation in the European Union, from 2000 to 2060. *Eur Heart J* 2013; **34**: 2746–51. <https://doi.org/10.1093/eurheartj/ehz280>
 38. Colilla S, Crow A, Petkun W, Singer DE, Simon T, Liu X. Estimates of current and future incidence and prevalence of atrial fibrillation in the U.S. adult population. *Am J Cardiol* 2013; **112**: 1142–47. Available from: <https://linkinghub.elsevier.com/retrieve/pii/S0002914913012885>
 39. Jaïs P, Cauchemez B, Macle L, Daoud E, Khairy P, Subbiah R, et al. Catheter ablation versus antiarrhythmic drugs for atrial fibrillation. *Circulation* 2008; **118**: 2498–2505. <https://doi.org/10.1161/CIRCULATIONAHA.108.772582>
 40. Kuck K-H, Hoffmann BA, Ernst S, Wegscheider K, Treszl A, Metzner A, et al. Impact of complete versus incomplete Circumferential lines around the pulmonary veins during catheter ablation of Paroxysmal atrial fibrillation. *Circ: Arrhythmia and Electrophysiology* 2016; **9**(1). <https://doi.org/10.1161/CIRCEP.115.003337>
 41. Kircher S, Arya A, Altmann D, Rolf S, Bollmann A, Sommer P, et al. Individually tailored vs. Standardized substrate modification during radiofrequency catheter ablation for atrial fibrillation: A randomized study. *Europace* 2018; **20**: 1766–75. <https://doi.org/10.1093/europace/eux310>
 42. Blomström-Lundqvist C, Gizurarson S, Schwieler J, Jensen SM, Bergfeldt L, Kenneback G, et al. Effect of catheter ablation vs antiarrhythmic medication on quality of life in patients with atrial fibrillation. *JAMA* 2019; **321**: 1059–68. <https://doi.org/10.1001/jama.2019.0335>
 43. Packer DL, Mark DB, Robb RA, Monahan KH, Bahnson TD, Poole JE, et al. Effect of catheter ablation vs antiarrhythmic drug therapy on mortality, stroke, bleeding, and cardiac arrest among patients with atrial fibrillation. *JAMA* 2019; **321**: 1261–74. <https://doi.org/10.1001/jama.2019.0693>
 44. Carpen M, Matkins J, Syros G, Gorev MV, Alikhani Z, Wylie JV, et al. First experience of 3D rotational angiography fusion with Navx Electroanatomical mapping to guide catheter ablation of atrial fibrillation. *Heart Rhythm* 2013; **10**: 422–27. <https://doi.org/10.1016/j.hrthm.2012.11.004>
 45. Emmert MY, Puippe G, Baumüller S, Alkadhhi H, Landmesser U, Plass A, et al. Safe, effective and durable Epicardial left atrial Appendage clip occlusion in patients with atrial fibrillation undergoing cardiac surgery: first long-term results from a prospective device trial. *Eur J Cardiothorac Surg* 2014; **45**: 126–31. <https://doi.org/10.1093/ejcts/ezt204>
 46. Caliskan E, Cox JL, Holmes DR Jr, Meier B, Lakkireddy DR, Falk V, et al. Interventional and surgical occlusion of the left atrial appendage. *Nat Rev Cardiol* 2017; **14**: 727–43. <https://doi.org/10.1038/nrcardio.2017.107>
 47. Kirchhof P, Benussi S, Kotecha D, Ahlsson A, Atar D, Casadei B, et al. ESC guidelines for the management of atrial fibrillation developed in collaboration with EACTS. *Europace* 2016; **18**: 1609–78. <https://doi.org/10.1093/europace/euw295>
 48. Yu S, Zhang H, Li H. Cardiac computed tomography versus Transesophageal echocardiography for the detection of left

- atrial Appendage thrombus: A systemic review and meta-analysis. *J Am Heart Assoc* 2021; **10**. <https://doi.org/10.1161/JAHA.121.022505>
49. Quintana RA, Dong T, Vajapey R, Reyalde R, Kwon DH, Harb S, et al. Preprocedural Multimodality imaging in atrial fibrillation. *Circ Cardiovasc Imaging* 2022; **15**(10): e014386. <https://doi.org/10.1161/CIRCIMAGING.122.014386>
 50. Glikson M, Wolff R, Hindricks G, Mandrola J, Camm AJ, Lip GYH, et al. EHRA/EAPCI expert consensus statement on catheter-based left atrial Appendage occlusion - an update. *EuroIntervention* 2020; **15**: 1133–80. https://doi.org/10.4244/EIJY19M08_01
 51. Al-Kassou B, Tzikas A, Stock F, Neikes F, Völz A, Omran H. A comparison of two-dimensional and real-time 3D Transoesophageal echocardiography and angiography for assessing the left atrial Appendage anatomy for SIZING a left atrial Appendage occlusion system: Impact of volume loading. *EuroIntervention* 2017; **12**: 2083–91. <https://doi.org/10.4244/EIJ-D-15-00543>
 52. Goitein O, Fink N, Hay I, Di Segni E, Guetta V, Goitein D, et al. Cardiac CT angiography (CCTA) predicts left atrial Appendage Occluder device size and procedure outcome. *Int J Cardiovasc Imaging* 2017; **33**: 739–47. <https://doi.org/10.1007/s10554-016-1050-6>
 53. Saw J, Fahmy P, Spencer R, Prakash R, McLaughlin P, Nicolaou S, et al. Comparing measurements of CT angiography, TEE, and Fluoroscopy of the left atrial Appendage for percutaneous closure. *J Cardiovasc Electrophysiol* 2016; **27**: 414–22. <https://doi.org/10.1111/jce.12909>
 54. Wang DD, Eng M, Kupsky D, Myers E, Forbes M, Rahman M, et al. Application of 3-dimensional computed Tomographic image guidance to WATCHMAN implantation and impact on early operator learning curve. *JACC Cardiovasc Interv* 2016; **9**: 2329–40. <https://doi.org/10.1016/j.jcin.2016.07.038>
 55. Cleland JGF, Daubert J-C, Erdmann E, Freemantle N, Gras D, Kappenberger L, et al. The effect of cardiac Resynchronization on morbidity and mortality in heart failure. *N Engl J Med* 2005; **352**: 1539–49. <https://doi.org/10.1056/NEJMoa050496>
 56. Ansalone G, Giannantoni P, Ricci R, Trambaiolo P, Fedele F, Santini M. Doppler myocardial imaging to evaluate the effectiveness of pacing sites in patients receiving biventricular pacing. *Journal of the American College of Cardiology* 2002; **39**: 489–99. [https://doi.org/10.1016/S0735-1097\(01\)01772-7](https://doi.org/10.1016/S0735-1097(01)01772-7)
 57. Sommer A, Kronborg MB, Nørgaard BL, Poulsen SH, Bouchelouche K, Böttcher M, et al. Multimodality imaging-guided left ventricular lead placement in cardiac resynchronization therapy: A randomized controlled trial. *Eur J Heart Fail* 2016; **18**: 1365–74. <https://doi.org/10.1002/ejhf.530>
 58. Mehta VS, Ayis S, Elliott MK, Wijesuriya N, Kardaman N, Gould J, et al. The role of guidance in delivering cardiac resynchronization therapy: A systematic review and network meta-analysis. *Heart Rhythm O2* 2022; **3**: 482–92. <https://doi.org/10.1016/j.hroo.2022.07.005>
 59. Abadia AF, van Assen M, Martin SS, Vingiani V, Griffith LP, Giovagnoli DA, et al. Myocardial extracellular volume fraction to differentiate healthy from Cardiomyopathic myocardium using dual-source dual-energy CT. *J Cardiovasc Comput Tomogr* 2020; **14**: 162–67. <https://doi.org/10.1016/j.jcct.2019.09.008>
 60. Bandula S, White SK, Flett AS, Lawrence D, Pugliese F, Ashworth MT, et al. Measurement of myocardial extracellular volume fraction by using equilibrium contrast-enhanced CT: validation against histologic findings. *Radiology* 2013; **269**: 396–403. <https://doi.org/10.1148/radiol.13130130>
 61. Buss SJ, Schulz F, Wolf D, Hosch W, Galuschky C, Schummers G, et al. Quantitative analysis of left ventricular Dyssynchrony using cardiac computed tomography versus three-dimensional echocardiography. *Eur Radiol* 2012; **22**: 1303–9. <https://doi.org/10.1007/s00330-011-2375-0>
 62. Truong QA, Singh JP, Cannon CP, Sarwar A, Nasir K, Auricchio A, et al. Quantitative analysis of Intraventricular Dyssynchrony using wall thickness by Multidetector computed tomography. *JACC Cardiovasc Imaging* 2008; **1**: 772–81. <https://doi.org/10.1016/j.jcmg.2008.07.014>
 63. Agudelo VH, Millán X, Li C-H, Moustafa A-H, Asmarats L, Serra A, et al. Prevalence, mechanisms and impact of residual Patency and device-related thrombosis following left atrial Appendage occlusion: A computed tomography analysis. *EuroIntervention* 2021; **17**: e944–52. <https://doi.org/10.4244/EIJ-D-21-00320>
 64. Pracon R, Bangalore S, Dzielinska Z, Konka M, Kepka C, Kruk M, et al. Device thrombosis after percutaneous left atrial Appendage occlusion is related to patient and procedural characteristics but not to duration of Postimplantation dual antiplatelet therapy. *Circ Cardiovasc Interv* 2018; **11**(3): e005997. <https://doi.org/10.1161/CIRCINTERVENTIONS.117.005997>
 65. Dong J, Calkins H. Technology insight: Catheter ablation of the pulmonary veins in the treatment of atrial fibrillation. *Nat Clin Pract Cardiovasc Med* 2005; **2**: 159–66. <https://doi.org/10.1038/ncpcardio0137>
 66. Sharma K, Brinker JA, Henrikson CA. Computed tomography imaging in atrial fibrillation ablation. *J Atr Fibrillation* 2011; **4**: 319: 319. <https://doi.org/10.4022/jafib.319>
 67. Lee HG, Shim J, Choi JI, Kim YH, Oh YW, Hwang SH. Use of cardiac computed tomography and magnetic resonance imaging in case management of atrial fibrillation with catheter ablation. *Korean J Radiol* 2019; **20**: 695–708. <https://doi.org/10.3348/kjr.2018.0774>
 68. Arbelo E, Brugada J, Blomström-Lundqvist C, Laroche C, Kautzner J, Pokushalov E, et al. Contemporary management of patients undergoing atrial fibrillation ablation: In-hospital and 1-year follow-up findings from the ESC-EHRA atrial fibrillation ablation long-term Registry. *Eur Heart J* 2017; **38**: 1303–16. <https://doi.org/10.1093/eurheartj/ehw564>
 69. Pappone C, Vicedomini G, Santinelli V. Atrio-esophageal fistula after AF ablation: Pathophysiology, prevention & treatment. *J Atr Fibrillation* 2013; **6**: 860: 860. <https://doi.org/10.4022/jafib.860>
 70. Berger WR, Meulendijks ER, Limpens J, van den Berg NWE, Neefs J, Driessen AHG, et al. Persistent atrial fibrillation: A systematic review and meta-analysis of invasive strategies. *International Journal of Cardiology* 2019; **278**: 137–43. <https://doi.org/10.1016/j.ijcard.2018.11.127>
 71. Saw J, Fahmy P, DeJong P, Lempereur M, Spencer R, Tsang M, et al. Cardiac CT angiography for device surveillance after endovascular left atrial appendage closure. *Eur Heart J Cardiovasc Imaging* 2015; **16**: 1198–1206. <https://doi.org/10.1093/ehjci/jev067>
 72. Boersma LV, Ince H, Kische S, Pokushalov E, Schmitz T, Schmidt B, et al. Efficacy and safety of left atrial Appendage closure with WATCHMAN in patients with or without Contraindication to oral anticoagulation: 1-year follow-up outcome data of the EWOLUTION trial. *Heart Rhythm* 2017; **14**: 1302–8. <https://doi.org/10.1016/j.hrthm.2017.05.038>
 73. Viles-Gonzalez JF, Kar S, Douglas P, Dukkupati S, Feldman T, Horton R, et al. The clinical impact of incomplete left atrial appendage closure with the Watchman device in patients with atrial fibrillation. *Journal of the American College of Cardiology* 2012; **59**: 923–29. <https://doi.org/10.1016/j.jacc.2011.11.028>

74. Qamar SR, Jalal S, Nicolaou S, Tsang M, Gilhofer T, Saw J. Comparison of cardiac computed tomography angiography and transoesophageal echocardiography for device surveillance after left atrial appendage closure. *EuroIntervention* 2019; **15**: 663–70. <https://doi.org/10.4244/EIJ-D-18-01107>
75. Lindner S, Behnes M, Wenke A, Sartorius B, Ansari U, Akin M, et al. Assessment of peri-device leaks after interventional left atrial appendage closure using standardized imaging by cardiac computed tomography angiography. *Int J Cardiovasc Imaging* 2019; **35**: 725–31. <https://doi.org/10.1007/s10554-018-1493-z>
76. Korsholm K, Jensen JM, Nørgaard BL, Samaras A, Saw J, Berti S, et al. Peridevice leak following Amplatzer left atrial Appendage occlusion: Cardiac computed tomography classification and clinical outcomes. *JACC Cardiovasc Interv* 2021; **14**: 83–93. <https://doi.org/10.1016/j.jcin.2020.10.034>
77. Lempereur M, Aminian A, Saw J. Rebuttal with regards to "device-associated thrombus formation after left atrial Appendage occlusion: A systematic review of events reported with the Watchman, the Amplatzer cardiac plug and the amulet. *Catheter Cardiovasc Interv* 2018; **92**: E216–17. <https://doi.org/10.1002/ccd.27135>
78. Reddy VY, Holmes D, Doshi SK, Neuzil P, Kar S. Safety of percutaneous left atrial Appendage closure. *Circulation* 2011; **123**: 417–24. <https://doi.org/10.1161/CIRCULATIONAHA.110.976449>
79. Landmesser U, Schmidt B, Nielsen-Kudsk JE, Lam SCC, Park J-W, Tarantini G, et al. Left atrial Appendage occlusion with the AMPLATZER amulet device: Periprocedural and early clinical/Echocardiographic data from a global prospective observational study. *EuroIntervention* 2017; **13**: 867–76. <https://doi.org/10.4244/EIJ-D-17-00493>
80. Simard TJ, Hibbert B, Alkhouli MA, Abraham NS, Holmes DR. Device-related thrombus following left atrial Appendage occlusion. *EuroIntervention* 2022; **18**: 224–32. <https://doi.org/10.4244/EIJ-D-21-01010>
81. Korsholm K, Jensen JM, Nørgaard BL, Nielsen-Kudsk JE. Detection of device-related thrombosis following left atrial appendage occlusion. *Circ Cardiovascular Interventions* 2019; **12**(9). <https://doi.org/10.1161/CIRCINTERVENTIONS.119.008112>